

Noise at a Fermi-edge singularity

N. Maire^{1,*}, F. Hohls¹, T. Lüdtkke¹, K. Pierz², and R. J. Haug¹

¹*Institut für Festkörperphysik, Universität Hannover, Appelstr. 2, D-30167 Hannover, Germany*

²*Physikalisch-Technische Bundesanstalt, Bundesallee 100, D-38116 Braunschweig, Germany*

(Dated: September 23, 2018)

We present noise measurements of self-assembled InAs quantum dots at high magnetic fields. In comparison to I-V characteristics at zero magnetic field we notice a strong current overshoot which is due to a Fermi-edge singularity. We observe an enhanced suppression in the shot noise power simultaneous to the current overshoot which is attributed to the electron-electron interaction in the Fermi-edge singularity.

PACS numbers: 73.63.Kv, 73.40.Gk, 72.70.+m

The measurement of shot noise provides information that cannot be extracted from conductance measurements alone [1]. It has its origin in time dependent fluctuations of the electrical current due to the discreteness of the charge. For an uncorrelated flow of electrons the shot noise power S induced by individual tunneling events is proportional to the stationary current I and the absolute charge of the electrons, $S = 2eI$ [2]. Interactions between the electrons e.g. Coulomb interaction or Pauli exclusion principle can reduce the shot noise power [3, 4]. For zero dimensional states, so called quantum dots, it has been shown both theoretically and experimentally that the shot noise power S is suppressed down to half its normal value, $[5, 6, 7, 8]$, $eI \leq S \leq 2eI$. Recently deviations in the shot noise power have been reported due to certain electron-electron interaction effects such as Kondo effect [9, 10, 11] or cotunneling [12].

Motivated by these results we present temperature dependent noise measurements of self-assembled InAs quantum dots under the influence of a high magnetic field leading to another electron-electron interaction effect, a so-called Fermi-edge singularity effect. Its dominant feature is a strong overshoot in the current at certain values of the bias voltage consistent with other tunneling experiments at a localized impurity [13] or at InAs quantum dots [14, 15]. We find that this overshoot is accompanied by a surprising additional suppression of the measured shot noise.

The active part of the investigated sample consists of a GaAs-AlAs-GaAs heterostructure. N -doped GaAs acts as 3d emitter and collector. Situated inside the AlAs are 1.8 monolayers InAs. Due to the Stranski-Krastanov growth mechanism InAs quantum dots (QD) are formed. The lower and upper AlAs tunneling barriers are 4 and 6 nm thick, respectively. Since transmission electron microscopy images show that the QDs have a height of 2-3 nm the effective thickness of the AlAs barrier on top of the QDs is reduced to 3-4 nm.

The sample is inserted into a ^3He system. This allows us to reach temperatures down to $T = 300$ mK and

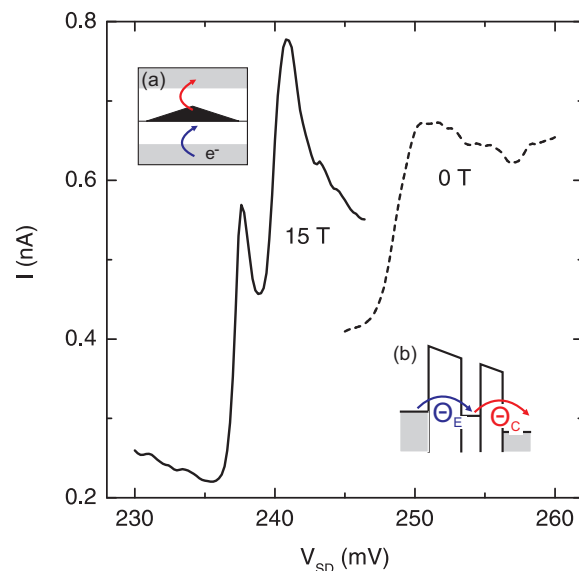


FIG. 1: I-V characteristic of a current step at 0 T (dashed line) and at 15 T (solid line).

Inset (a): Schematic of the tunneling direction of the electrons through the pyramidal shaped quantum dots.

Inset (b): Schematic of the corresponding band diagram when resonant tunneling condition is achieved.

magnetic fields up to 15 T. A DC bias is applied to the sample and the current is amplified by a low noise current amplifier with a bandwidth of 20 kHz. The DC part is monitored by a voltmeter. A fast-Fourier-transform analyzer measures the noise spectra.

The I-V characteristic of the sample shows distinct steps. These steps correspond to resonant tunneling through individual quantum dots [16]. It should be noted that at zero bias the ground state energy of the quantum dots is well above the Fermi energy in the leads [8]. Resonant tunneling only sets in when the applied bias voltage is sufficiently large to bring the quantum dots' ground state energy on par with the emitter Fermi edge. One of these steps due to resonant tunneling is shown in Fig. 1 (dashed line). The applied positive bias voltage corresponds to the tunneling direction depicted in the inset (a). The electrons first tunnel through the 4 nm thick

*Electronic address: maire@nano.uni-hannover.de

barrier into the dot and leave it through the thinner 3-4 nm barrier. So we expect the tunneling rate Θ_C out of the dot into the collector to be higher than the emitter rate Θ_E out of the emitter into the dot. We point out the fact that transport measurements at a sample from the same wafer structure also showed characteristics of a much higher collector tunneling rate Θ_C [19]. The fact that we observe strong fluctuations in the I-V characteristic stemming from fluctuations of the local density of states in the emitter [17] strengthens the expectation of asymmetric tunneling rates with a much higher collector tunneling rate Θ_C . A schematic view of the corresponding band structure is shown in inset (b).

Also shown is the same current step at a high magnetic field of 15 T (solid line). The features discussed in the following were also seen down to magnetic fields of ≈ 12 T, 15 T was chosen for the most distinct characteristics.

At this large magnetic field the resonance is shifted slightly to lower bias voltages due to the fact that the emitter electrons have been redistributed into the lowest Landau level leading to a lower emitter Fermi energy E_F . It has split into two peaks due to Zeeman splitting of the ground state of the quantum dot.

The more interesting feature is the strong peak like current overshoot at the steps. The absolute current at 15 T doubles compared to 0 T. The likely origin of this overshoot is the Fermi-edge singularity effect which is an interaction effect between the localized electron on the dot and the electrons near the Fermi edge of the emitter. One signature of the Fermi-edge singularity is a temperature dependence of the current step height ΔI following the equation [15]

$$\ln(\Delta I) \sim -\gamma \cdot \ln(T). \quad (1)$$

In Fig. 2 the current step at 15 T is shown for five different temperatures ranging from $T = 0.3$ K to $T = 1$ K. The temperature dependent height of the peaks is clearly visible. In the inset of Fig. 2 a plot of $\ln(\Delta I)$ of the first peak at ≈ 238 mV vs. $-\ln(T)$ is shown. A fit using Eq. (1) yields $\gamma = 0.40 \pm 0.03$. For similar measurements of a Fermi-edge singularity at InAs quantum dots $\gamma = 0.43$ was obtained [15].

Another characteristic attribute of a Fermi-edge singularity effect is a voltage dependence of the current given by [13]

$$I \sim (V_{SD} - V_{Th})^{-\gamma} \quad (2)$$

V_{Th} corresponds to the bias voltage at which the Fermi energy of the emitter is in resonance with the ground state of the dot. From the I-V characteristics for different temperatures we determine $V_{Th} = 237.4$ mV. A fit of the 0.3 K data using Eq. (2) with fixed V_{Th} yields $\gamma = 0.47 \pm 0.01$ in fair agreement with the exponent determined above. This fit is shown by the thick line in Fig. 2 and matches the measurement well. We conclude that this current overshoot is indeed caused by a Fermi-edge singularity effect. A more sophisticated analysis of

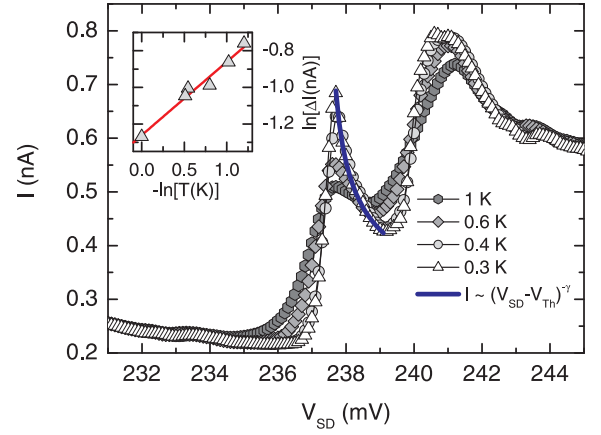


FIG. 2: I-V characteristic of the current step at $B = 15$ T for five different temperatures. Thick line: Fit using Eq. (2). Inset: Current step heights ΔI for different temperatures (symbols) and corresponding fit using Eq. (1) (line).

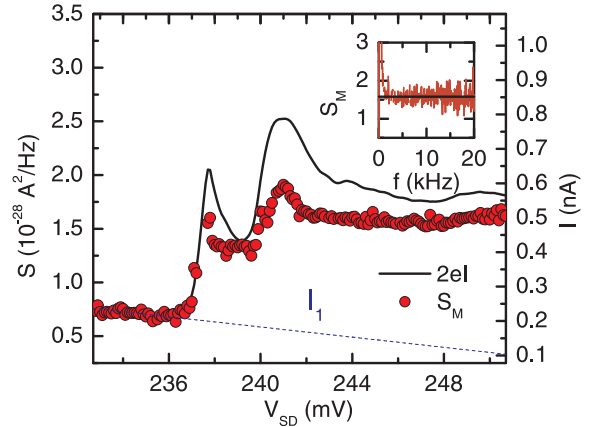


FIG. 3: Measured shot noise power S_M (filled dots, left axis) and current I (solid line, right axis). The scale on the right axis was chosen in such a way that the solid line corresponds on the left axis to the shot noise power of a single tunneling barrier, $S = 2eI$. Also shown is the linear fitted background current I_1 (dashed line, right axis). Inset: shot noise spectrum for $V_{SD} = 244$ mV.

the Fermi-edge singularity effect at a current step can be found in Ref. [18]

We will now analyze the noise characteristic of this particular electron-electron interaction effect: At high frequencies the measured noise power density is frequency independent as expected for shot noise, while at low frequencies additional $1/f$ noise appears. To remove the $1/f$ part, a $A/f + S_M$ fit is carried out, S_M being the resulting average shot noise power. A sample spectrum is shown in the right inset of Fig. 3. For high differential source conductance we additionally have to account for the input voltage noise of the amplifier which adds a term B/f^β with $\beta \approx 2$. We include this term into the fit for the steep risers at $V_{SD} \approx 237$ mV and $V_{SD} \approx 240$ mV. S_M is shown in Fig. 3 by the filled dots. Comparing S_M

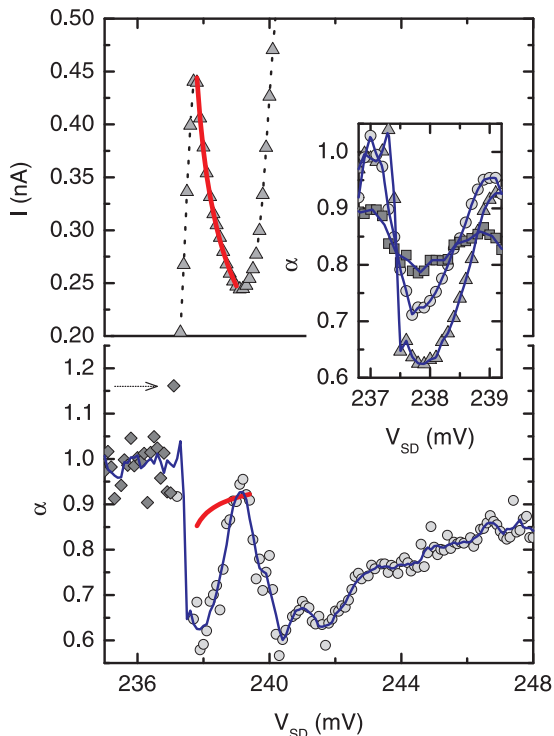


FIG. 4: Fano factor α (left axis) at 0.4 K using $\alpha = S_M/2eI$ (diamonds) and α_1 (see text, circles). The drawn through line is a boxcar average. The thick solid line is a test of eq. (3) (see text). Also shown is the corresponding current I (upper panel) and its fit using eq. (4) (see text, solid line). Inset: boxcar averages of the Fano factor for 0.4 (triangles), 0.6 (circles) and 1 K (squares). The drawn through lines act as guides to the eye.

to the full shot noise $S = 2eI$ of single barrier tunneling we find the expected suppression of shot noise on resonance.

In a semiclassical picture the suppression of shot noise has its origin in electron interaction effects such as Coulomb blockade and Pauli exclusion principle. An emitter electron cannot enter the dot when it is already occupied by another electron. This anticorrelation then leads to the afore mentioned suppressed shot noise compared to a single tunneling barrier. To better characterize the degree of shot noise suppression the Fano factor $\alpha = S_M/2eI$ is introduced. For zero temperature the Fano factor α for a single ground state can be described by [6]

$$\alpha = 1 - \frac{2\Theta_E\Theta_C}{(\Theta_E + \Theta_C)^2} \quad (3)$$

with the emitter-dot tunneling rate Θ_E and collector-dot tunneling rate Θ_C . For a quantum dot α is expected to be in the range of 0.5 to 1, 0.5 for symmetrical barriers ($\Theta_E = \Theta_C$) and close to 1 for very asymmetric barriers.

In Fig. 4 the measured Fano factor is shown. Below 237 mV $\alpha \approx 1$ is observed. This can be explained in the following way: At ≈ 220 mV resonant tunneling through

another quantum dot sets in. For resonant transport at voltages sufficiently far away from the onset voltage a Fano factor of $\alpha \approx 1$ is expected [19]. We see an enhanced shot noise ($\alpha = 1.16$, see arrow in Fig. 4) just at the beginning of the current step at 237.1 mV. The origin of this overshoot is unclear but we observe it consistently for each measurement. With increasing temperatures the overshoot gets less until it has completely vanished at 1 K. Super Poissonian noise has also been recently observed at different quantum dot systems [20, 21].

To extract the Fano factor originating only from the quantum dot participating in the resonant tunneling process with the Fermi-edge singularity effect we have to subtract the influence of the other afore mentioned dot being resonant at ≈ 220 mV. The contribution $\alpha_{1,2}$ of the two quantum dots to the Fano factor is given by their fractions $I_{1,2}$ of the overall current I [8, 22]: A linear fit of the current I_1 of the dot with resonance at 220 mV is depicted by the dashed line in Fig. 3. If we now calculate α_2 with an $\alpha_1 = 1$ and the linear fitted current I_1 we get the Fano factor given by the circles in Fig. 4. The line is a 3 pt. boxcar average of these data.

As can be seen the Fano factor α exhibits a very sharp dip at the onset of the current step ($V_{SD} = 237$ mV) with a maximum suppression at the voltage position of the current peak. For further increased voltage we observe a strong rise of α in parallel to the large decrease in current. The pattern is repeated when the upper Zeeman level of the quantum dot comes into resonance at $V_{SD} = 240$ mV. We will restrict the following discussion of the Fano factor to the range $V_{SD} \leq 239$ mV where the second Zeeman level can be safely ignored as only a very small fraction of the current is carried by this second level.

The initial drop of α can be qualitatively explained following Ref. [19]: At the onset of resonant tunneling only the highest energetic emitter electrons in the tail of the emitter Fermi distribution function f_E can participate in a resonant tunneling process and the effective tunneling rate can be written as $\Theta_E = \Theta_E^0 f_E$ with $f_E \ll 1$ and thus $\Theta_E \ll \Theta_C$. Therefore we start with $\alpha \approx 1$. With increasing bias voltage the energy level of the dot is shifted downwards with respect to the Fermi level of the emitter and $f_E = 0 \rightarrow 1$. Θ_E increases accordingly, leading to a rise in the current and with Eq. (3) to a decrease of the Fano factor.

In our previous measurements of similar devices at $B = 0$ we have shown that the initial drop of the Fano factor is followed by a gentle rise over several ten mV which mirrors the density of states in the emitter [19]. In our measurement here for 15 T we observe a change of α on a totally different voltage scale: The Fano factor rises rapidly from $\alpha = 0.58$ at 237.9 mV to $\alpha = 0.91$ at 238.9 mV. Both Fano factor and current change dramatically within a voltage range of only 1 mV!

We indeed anticipate a rapid change near the Fermi energy in the presence of a Fermi-edge singularity. We will now try whether the measured current I and Fano factor α can be modeled by the introduction of an interaction

enhanced emitter tunneling rate Θ_E into the semiclassical relations for I and α . In the zero temperature limit Θ_E is predicted to follow [23]:

$$\Theta_E(V_{SD}) = \Theta_E^0 \left(\frac{D}{e(V_{SD} - V_{Th})} \right)^\gamma \quad (4)$$

for a voltage near but not too close to the threshold voltage V_{Th} . Following Ref. [23] the increase of the current peak can then be described by

$$I = e \frac{\Theta_C \Theta_E(V_{SD})}{\Theta_C + \Theta_E(V_{SD})} \quad (5)$$

Due to the high bias the change of the collector tunneling rate Θ_C is negligible in the range of interest [19], and we determine it far away from the resonances where the effect of the Fermi-edge singularity is negligible [$\Theta_C = 3.4 \cdot 10^{10} \text{ s}^{-1}$ at $V_{SD} = 248 \text{ mV}$]. Inserting Θ_C in Eq. (5) and fitting the first current peak [$V_{Th} = 237.4 \text{ mV}$ fixed; $\gamma = 0.45$ and $\Theta_E^0(D/e)^\gamma = 8.4 \cdot 10^7 \text{ V}^\gamma/\text{s}$ fitted] gives sound agreement with the measurement as depicted in Fig. 4 by the thick solid line in the upper panel.

We can now insert the above determined interaction enhanced and voltage dependent tunneling rate $\Theta_E(V_{SD})$ into the semiclassical equation Eq. (3). The resulting prediction for α is depicted by the thick solid line in the lower panel of Fig. 4. The values calculated at some distance to the Fermi-edge singularity where the interaction effects are weak are in reasonable agreement with our measurement (e.g. $\alpha = 0.92$ at $V_{SD} = 239.4 \text{ mV}$). However, near to the Fermi-edge singularity we observe a significant discrepancy: The calculated shot noise suppression of $\alpha = 0.86$ at $V_{SD} = 237.9 \text{ mV}$ falls way short of the measured strong suppression $\alpha = 0.58$; the measured change of α is much more rapid than the calculated one.

Thus we find that Eq. (3) is not applicable near the Fermi edge singularity. The Fano factor cannot be accounted for by just inserting an interaction enhanced tunneling rate Θ_E into a relation that was deduced in a sequential tunneling picture. Instead we observe a strongly

reduced Fano factor hinting onto additional anticorrelations of the tunneling events due to the interaction between lead and dot at the Fermi edge singularity.

The strong impact of the Fermi-edge singularity on the shot noise is further confirmed by the influence of temperature; the inset of Fig. 4 shows the temperature dependence of the Fano factor near the resonance. We observe a much stronger temperature dependence than expected when just using the changing Fermi function f_E in the effective tunneling rate $\Theta_E = \Theta_E^0 f_E$ at the step edge [19].

We conclude that the current noise in the regime of the Fermi-edge singularity reveals the coherent nature of the interaction between the emitter and the dot. Only a theory that accounts for this interaction will be able to describe the shot noise near the singularity. The relevance of interactions between the lead and the dot were pointed out for quantum dots in the regime of large tunnel coupling where the Kondo effect is observed. A number of *theoretical* papers [9, 10, 11] emphasized the importance of noise measurements to probe the Kondo regime, but due to the difficulty of the measurement experimental data in this regime are still missing. The need to go beyond sequential tunneling in a regime of lower coupling was demonstrated in *calculations* for an Anderson-impurity model with finite spin splitting [12] and now awaits experimental verification. For both the above mentioned Kondo and cotunneling regime the spin degree of freedom on the dot was essential. In contrast our experiment demonstrates the relevance of interaction for a single level system with only one spin species involved. Thus beside *experimentally* demonstrating the relevance of shot noise to examine the dot-lead interaction we also reveal the importance of current correlations in a new regime.

In summary we have measured the shot noise at a Fermi-edge singularity. We have observed strong shot noise suppression which we attribute to strong interaction between lead and dot at the Fermi-edge singularity.

We acknowledge financial support from BMBF via the program "NanoQUIT".

-
- [1] Y. M. Blanter and M. Büttiker, Phys. Rep. **336**, 1 (2000).
 - [2] W. Schottky, Ann. Phys. (Leipzig) **57**, 541 (1918).
 - [3] Y. P. Li, A. Zaslavsky, D. C. Tsui, M. Santos, and M. Shayegan, Phys. Rev. B **41**, 8388 (1990).
 - [4] H. C. Liu, J. Li, G. C. Aers, C. R. Leavens, M. Buchanan, and Z. R. Wasilewski, Phys. Rev. B **51**, 5116 (1995).
 - [5] H. Birk, M. J. M. de Jong, and C. Schönenberger, Phys. Rev. Lett. **75**, 1610 (1995).
 - [6] L. Y. Chen and C. S. Ting, Phys. Rev. B **43**, 4534 (1991).
 - [7] J. H. Davies, P. Hyldgaard, S. Hershfield, and J. W. Wilkins, Phys. Rev. B **46**, 9620 (1992).
 - [8] A. Nauen, I. Hapke-Wurst, F. Hohls, U. Zeitler, R. J. Haug, and K. Pierz, Phys. Rev. B **66**, 161303(R) (2002).
 - [9] Y. Meir and A. Golub, Phys. Rev. Lett. **88**, 116802 (2002).
 - [10] R. Lopez and D. Sanchez, Phys. Rev. Lett. **90**, 116602 (2003).
 - [11] E. Sela, Y. Oreg, F. von Oppen, and J. Koch, Phys. Rev. Lett. **97**, 086601 (2006).
 - [12] A. Thielmann, M. H. Hettler, J. König, and G. Schön, Phys. Rev. Lett. **95**, 146806 (2005).
 - [13] A. K. Geim, P. C. Main, N. La Scala Jr, L. Eaves, T. J. Foster, P. H. Beton, J. W. Sakai, F. W. Sheard, M. Henini, G. Hill, and M. A. Pate, Phys. Rev. Lett. **72**, 2061 (1994).
 - [14] K. A. Benedict, A. S. G. Thornton, T. Ihn, P. C. Main, L. Eaves, and M. Henini, Physica B **256-258**, 519 (1998).
 - [15] I. Hapke-Wurst, U. Zeitler, H. Frahm, A. G. M. Jansen,

- R. J. Haug, and K. Pierz, Phys. Rev. B **62**, 12621 (2000).
- [16] I. Hapke-Wurst, U. Zeitler, U. F. Keyser, R. J. Haug, K. Pierz, and Z. Ma, Appl. Phys. Lett. **82**, 1209 (2003).
- [17] T. Schmidt, R. J. Haug, V. I. Fal'ko, K. v. Klitzing, A. Förster, and H. Lüth, Europhys. Lett. **36**, 61 (1996).
- [18] H. Frahm, C. von Zobeltitz, N. Maire, and R. J. Haug, Phys. Rev. B. **74** 035329 2006.
- [19] A. Nauen, F. Hohls, N. Maire, K. Pierz, and R. J. Haug, Phys. Rev. B **70**, 033305 (2004).
- [20] P. Barthold, F. Hohls, N. Maire, K. Pierz, and R. J. Haug, Phys. Rev. Lett. **96**, 246804 (2006).
- [21] S. Gustavsson, R. Leturcq, B. Simović, R. Schleser, P. Studerus, T. Ihn, K. Ensslin, D. C. Driscoll, and A. C. Gossard, cond-mat/0605365.
- [22] G. Kiesslich, A. Wacker, E. Schöll, A. Nauen, F. Hohls, and R. J. Haug, phys. stat. sol. (c) **0**, 1293 (2003).
- [23] K. A. Matveev and A. I. Larkin, Phys. Rev. B **46**, 15337 (1992).